Spin Fluctuations in Sr_{2}RuO_{4} from Polarized Neutron Scattering: Implications for Superconductivity

P. Steffens, Y. Sidis, J. Kulda, Z. Q. Mao, Y. Maeno, I. I. Mazin, and M. Braden

Phys. Rev. Lett. **122**, 047004 — Published 1 February 2019

DOI: 10.1103/PhysRevLett.122.047004

Spin fluctuations in Sr_2RuO_4 from polarized neutron scattering: implications for superconductivity

P. Steffens,[1,2] Y. Sidis,[3] J. Kulda,[2] Z. Q. Mao,[4,5,6] Y. Maeno,[4] I.I. Mazin,[7] and M. Braden[1,*]

[1] *II. Physikalisches Institut, Universität zu Köln, Zülpicher Str. 77, D-50937 Köln, Germany*
[2] *Institut Laue Langevin,71 avenue des Martyrs, 38000 Grenoble, France*
[3] *Laboratoire Léon Brillouin, C.E.A./C.N.R.S., F-91191 Gif-sur-Yvette CEDEX, France*
[4] *Department of Physics, Graduate School of Science, Kyoto University, Kyoto 606-8502, Japan*
[5] *Department of Physics, Tulane University, New Orleans, LA 70118, USA*
[6] *Department of Physics, Pennsylvania State University, University Park, PA 16802, USA*
[7] *Code 6393, Naval Research Laboratory, Washington, District of Columbia 20375, USA*

Triplet pairing in Sr_2RuO_4 was initially suggested based on the hypothesis of strong ferromagnetic spin fluctuations. Using polarized inelastic neutron scattering, we accurately determine the full spectrum of spin fluctuations in Sr_2RuO_4. Besides the well-studied incommensurate magnetic fluctuations we do find a sizeable quasiferromagnetic signal, quantitatively consistent with all macroscopic and microscopic probes. We use this result to address the possibility of magnetically-driven triplet superconductivity in Sr_2RuO_4. We conclude that, even though the quasiferromagnetic signal is stronger and sharper than previously anticipated, spin fluctuations alone are not enough to generate a triplet state strengthening the need for additional interactions or an alternative pairing scenario.

Superconducting Sr_2RuO_4 [1–3] was proposed to be a solid-state analogue of He^3, *i. e.*, a triplet superconductor [4, 5], based on its proximity to $SrRuO_3$, a ferromagnetic (FM) metal. A simple model derived from the density-functional theory (DFT) for $SrRuO_3$, $CaRuO_3$ and $SrYRu_2O_6$ [6] ascribed the mass and spin susceptibility renormalization to FM fluctuations, and predicted a triplet pairing [5]. Experimental evidence pointing toward a particular (chiral-p) triplet was obtained, such as temperature-independent uniform susceptibility for the in-plane fields and time-reversal symmetry breaking [2, 7–9]. However, the dominant spin fluctuations in Sr_2RuO_4 are not FM (*i.e.* q=0), but incommensurate (IC) antiferromagnetic (AFM) [10, 11], and several experiments are inconsistent with either triplet states, or time-reversal breaking, or both [9]. Various theories were proposed to explain triplet pairing by incorporating higher-order vertex corrections [12, 13], the interplay of incommensurate charge and spin fluctuations [14] or orbital fluctuations [15, 16], arriving at different superconducting (SC) states. Even the question about which bands drive pairing remains controversial [17, 18].

The Fermi surface of Sr_2RuO_4 is known to tiny details [2, 19–21]. It has two quasi-one-dimensional (q1D), and one rather isotropic quasi-two-dimensional (q2D) sheets, derived from $d_{xz,yz}$ and d_{xy} orbitals, respectively. Sr_2RuO_4 exhibits an almost temperature independent normal-state susceptibility [22], which is enhanced by a factor ∼7 compared to the DFT value [23–25]. The enhancement factor of the IC fluctuations is even larger, ∼30 [11, 26, 27], since the bare susceptibility is larger [10]. Also the electronic specific heat coefficient of about 38 mJ/mol·K^2 is enhanced by a factor of ∼3, yielding a Wilson ratio of ∼2. Similarly, quantum oscillations show strong and band-dependent mass renormalizations, which can be explained by quasiferromagnetic (qFM) fluctuations [5], in the spirit of He^3, but also in terms of local Hund's rule fluctuations [28, 29].

Inelastic neutron scattering (INS) experiments detect strong IC spin fluctuations at $\mathbf{q}_{\rm IC}$=(±0.3,±0.3,q_l) [11, 26, 27, 30–33] arising from nesting in the q1D bands. Upon minor substitution with Ti or Ca this instability condenses into a static spin-density wave with the same $\mathbf{Q}$ [34–37]. INS also assesses the anisotropy of magnetic excitations, which is known to favor triplet pairing [38–40], and find it to be non-negligible, but still small [30]. Finally, recent high-resolution INS reveals that the nesting fluctuations do not change between the normal and superconducing states even for energies well below the SC gap [33]. The NMR relaxation rate, $1/T_1T$, probes the spin susceptibility $\chi''(\mathbf{q},\omega)/\omega$ integrated over the entire Brillouin zone, and exhibits the same temperature dependence as the INS nesting signal [11, 26, 41, 42], indicating that it is dominated by the latter. However, $1/T_1T$ also shows a weaker, temperature-independent offset, pointing to another contribution tentatively attributed to the FM response. This tendency towards ferromagnetism can be enhanced by Co [43] or Ca [44] substitution.

To this end, we have used polarized INS to search for the missing FM fluctuations in Sr_2RuO_4. The magnetic response consists of two components: a broad maximum around $\mathbf{q}$ = 0, which we will call qFM, and an IC, and much stronger, AFM component. We entered this full magnetic susceptibility into the BCS equations describing spin-fluctuation-induced SC pairing.

Because neutron polarization analysis suffers from a reduced intensity, we used a large sample of ten aligned crystals grown at Kyoto University [45] with a total volume of 2.2 cm^3 and a mosaic spread of 1.9(2) degrees. Experiments were performed on the spectrometer IN20

at the Institut Laue Langevin, for details see [46]. In general, neutron scattering only senses magnetic components that are polarized perpendicular to the scattering vector **Q**. The polarization analysis distinguishes spin-flip (SF_i with i=x, y, and z the direction of neutron polarization) and non-spin-flip (nSF_i) processes and adds further selection rules. Phonon scattering and nuclear Bragg peaks only contribute to the nSF_i channels, but magnetic scattering contributes to the SF_i channel when the magnetic component is perpendicular to the direction of neutron polarization, and to the nSF_i channel otherwise. We use the conventional coordinate system with **x** parallel to **Q**, **z** perpendicular to the scattering plane, and $\mathbf{y} = \mathbf{z} \times \mathbf{x}$.

Even with our large sample it was impossible to quantitatively analyze the qFM response by unpolarized INS, because it is too little structured in **q** space impeding a background (BG) determination, see supplemental material [46]. In contrast, the polarization analysis permits a direct BG subtraction at each point in **Q** and energy. For instance, 2I(SF_x)-I(SF_y)-I(SF_z) yields a BG-free total magnetic signal (up to a correction for the finite flipping ratio). Fig. 1 (b-c) shows a representative scan through both the IC and the FM **Q** positions. The full polarization analysis is shown for the SF (b) and the nSF (c) channels. The SF signals have been counted with better statistics, because the SF count rates always contain the magnetic signal and have a lower BG. Only the nSF_y and nSF_z channels contain a single magnetic component superposed with the larger nSF scattering, which contains all the phonon contributions. The appearance of the nesting signal in various channels is well confirmed; Fig. 1 (b) clearly shows the anisotropy of the IC nesting signal at $(-0.3, 0.7, 0)$ discussed in Ref. [30]. The sharp enhancement at $(0, 1, 0)$ is present only in the nSF channel, which proves its non-magnetic character (the longitudinal zone-boundary phonon) [47, 48]. The finite flipping ratio was determined on several phonon modes, which integrates the signal of all individual crystals, yielding values between 8 and 10. The final analysis only used the SF data, corrected by the average flipping ratio, because of their higher signal to BG ratio [49].

Polarized INS results displaying the average of two magnetic components (in-plane plus out-of-plane) are shown in Fig. 1 for T=1.6 K and in the supplemental material for T=150 K [46]. In order to compare scans taken at different but equivalent scattering vectors, a correction for the magnetic form factor has been applied. The observation of magnetic fluctuations in so many different scans unambiguously documents the existence of sizeable qFM fluctuations. The analysis furthermore yields the absolute scale of the magnetic response throughout the entire Brillouin zone, which allows us to construct a model for the full susceptibility $\chi''(\mathbf{q}, E)$. The calibration into absolute susceptibility units has been performed by the comparison with the scattering intensity arising from an acoustic phonon, similar to the procedure described

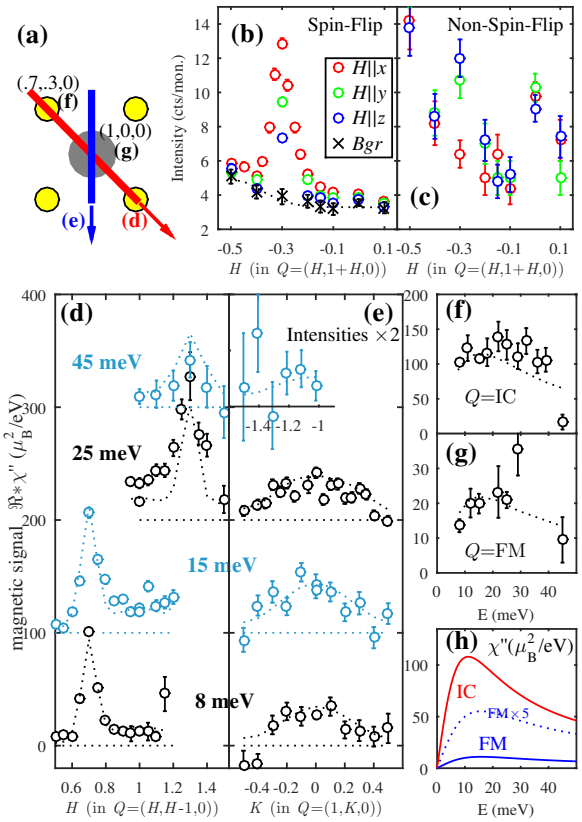

FIG. 1: (a) 2D reciprocal space of Sr_2RuO_4; qFM scattering is indicated by large (grey) discs and the IC signal by small (yellow) circles. Arrows show typical scan directions. (b-c) Diagonal scans at 8 meV and 1.6 K (across (-0.3,0.7,0) and (0,1,0)): (b) SF count rates, (c) nSF count rates. (d) Magnetic signal along diagonal scans at 1.6 K; note that the BG is eliminated through the polarization analysis. Scan paths are not identical, but all run through one $\mathbf{Q}_{IC}$ towards (1,0,0), see (a). The signal in (d-g) has been corrected for the magnetic form factor and the Bose factor and represents $\chi''(\mathbf{q}, E)$ convoluted with the resolution function, labelled $\Re * \chi''(\mathbf{q}, E)$. In (e) the results of the scans parallel to the a*/b* axes are shown. Energy scans at $\mathbf{Q}_{IC}$ and $\mathbf{Q}_{FM}$ are shown in (f) and (g), respectively. Lines in (d-g) denote the fitted model folded with the resolution. The unfolded incommensurate and qFM susceptibilities are shown in (h) (single component).

in Ref. 50. This calibration can be performed with high precision in the case of Sr_2RuO_4, because the phonon dispersion is well known and a lattice dynamical model exists that was used to calculate the phonon signal strength at finite propagation vectors [47, 48], while in most cases the $q \to 0$ limit is used as an approximation. Note, however, that the INS signal does not directly correspond to $\chi''(\mathbf{q}, E)$ but to its folding with the resolution function, $\Re * \chi''(\mathbf{q}, E)$, see Fig. 1 (d-g). Only if the resolution is much better than the typical variation of $\chi''(\mathbf{q}, E)$ the convolution has no visible effect.

The quantitative model fitted to the data consists of

TABLE I: (Upper part) Parameters of the $\chi''(\mathbf{q}, E)$ model for Sr_2RuO_4 refined with the polarized INS data for T=1.6 and 150 K. (Lower part) The largest triplet, T, and singlet, S, eigenvalues (in arbitrary units) of the interaction matrices V_s and V_t, respectively (Eq. 3), obtained for the isotropic susceptibility, $\chi'=\chi'(q,0)$ or for the anisotropic components χ'_{zz} and χ'_{ab}; the largest eigenvalues for qFM or IC fluctuations only are shown together with those for the total susceptibility.

T [K]	$\chi'_{\rm FM}$ [μ_B^2/eV]	W [r.l.u]	$\Gamma_{\rm FM}$ [eV]	$\chi'_{\rm IC}$ [μ_B^2/eV]	$\xi_{\rm IC}$ [Å]	$\Gamma_{\rm IC}$ [eV]
1.6	22±1	0.53±0.04	15.5±1.4	213±10	9.7±0.5	11.1±0.8
150	22±2	0.47±0.06	19.0±3.5	89±7	6.1±0.5	17.8±2.9

	qFM T	qFM S	IC T	IC S	total T	total S
χ'	10.6	0.21	16.8	94.8	18	87
χ'_{zz}	11.7	0.23	29.1	164.2	30.3	155.6
χ'_{ab}	9.6	0.19	9.7	54.7	11.3	48.3

two parts: the IC peaks centered at $\mathbf{Q}_{\rm IC}$ and the broad and weakly $\mathbf{q}$-dependent qFM part at the zone center. We write $\chi''(\mathbf{q}, E) = \chi''_{\rm IC}(\mathbf{q}, E) + \chi''_{\rm FM}(\mathbf{q}, E)$, where

$$\chi''_{\rm IC}(\mathbf{q}, E) = \chi'_{\rm IC} \frac{\Gamma_{\rm IC} \cdot E}{E^2 + \Gamma_{\rm IC}^2[1 + \xi_{\rm IC}^2(\frac{2\pi}{a}\Delta q)^2]^2} \quad (1)$$

is the single-relaxor formula with both $(\Gamma_{\mathbf{q}})^{-1}$ and $\chi'(\mathbf{q}, 0)$ decaying with the same correlation length $\xi_{\rm IC}$. Here $\Delta q = |\mathbf{q} - \mathbf{q}_{\rm IC}|$, and is measured in the reciprocal lattice units, (r.l.u.), equal to $2\pi/a$.

Equation (1) describes a typical magnetic response near an AFM instability [51]. The qFM term was described by a broad Gaussian, and its energy dependence in the single-relaxor form with the constant parameter $\Gamma_{\rm FM}$:

$$\chi''_{\rm FM}(q, E) = \chi'_{\rm FM} \cdot \frac{\Gamma_{\rm FM} \cdot E}{E^2 + \Gamma_{\rm FM}^2} \cdot \exp\left(-\frac{q^2}{W^2} 4\ln(2)\right) \quad (2)$$

and $\mathbf{q}$ is the distance to the nearest 2D Bragg point. The parameters resulting from a global fit to the whole data set are given in Table I [52]. The model susceptibility was convoluted with the spectrometer resolution using the reslib program package [53] and scaled through phonon scattering [48] yielding the lines in Fig. 1 (d-g).

The corresponding real part of the susceptibility at zero energy $\chi'(\mathbf{q}, E = 0)$, i.e. the amplitudes of the spectra at fixed $\mathbf{q}$, as well as $\chi''(\mathbf{q}, E)$ for $\mathbf{q}$ along the Brillouin zone diagonal are displayed in Fig. 2. The qFM signal shows no significant anisotropy and corresponds to the macroscopic susceptibility, which also exhibits only weak anisotropy [2, 3]. For the IC peak, the model describes the average of the in-plane and out-of-plane susceptibilities [30], with χ'_c (χ'_{ab}) slightly larger (smaller) than this value. The model was obtained by refining the only 6 parameters with the total set of 120

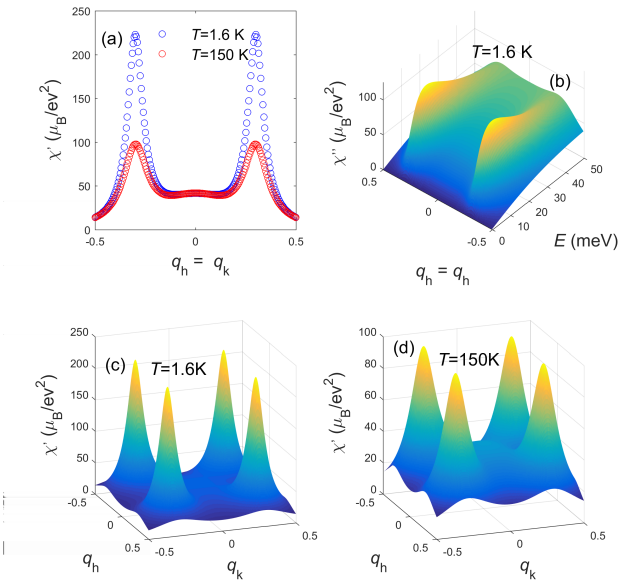

FIG. 2: The real part of the static susceptibility $\chi'(\mathbf{q}, E = 0)$ as described by eqs. (1,2) along the zone diagonal (a) and for the entire zone (c) at 1.6 K and (d) at 150 K; in (b) $\chi''(\mathbf{q}, E)$ is shown along the Brillouin zone diagonal.

independent data points at 1.6 K and 76 at 150 K. Thus obtained $\chi'_{\rm IC}$ and $\Gamma_{\rm IC}$ are somewhat higher than those extracted from unpolarized INS [11, 26]. The correlation length $\xi_{\rm IC}$ is less accurate but the qualitative decrease at higher temperature is unambiguous. In principle, one should consider the in-plane and out-of-plane components of the IC peak separately and then take their superposition, but the limited statistics does not allow for that. In contrast to the IC signal, the qFM one is basically temperature-independent, in agreement with the macroscopic measurement [22]. Thus, the qFM response becomes more visible at high temperatures. Note that, due to the simplicity of the model [52], the macroscopic susceptibility of $\sim$28 μ_B^2/eV·(f.u.) is smaller than in the model, $\sim$41 μ_B^2/eV·(f.u.).

The model $\chi''(\mathbf{q}, E)$ can also be successfully verified against $1/T_1T$ in NMR [41, 42, 54–57] and specific heat data [22, 58, 59], see supplemental material [46]. The impact of the qFM fluctuations must not be underestimated; because of the larger phase space, they yield about 85% of the specific-heat enhancement.

The qFM signal in Sr_2RuO_4 does not correspond to the paramagnon scattering expected close to a FM instability [51]; instead it can be viewed as as an AFM instability with a small but finite propagation vector near the Brillouin-zone center and a width that largely exceeds the length of the propagation vector. The superposition of several low-$\mathbf{q}$ contributions can result in the observed broad feature centered at $\mathbf{q}$=(0,0) and indeed several calculations of the q-dependent susceptibility in Sr_2RuO_4 reveal sharp features near (0.1,0.1,0) associated with the

γ band [60, 61, 67]. $Ca_{2-x}Sr_2RuO_4$ with $0.2 < x < 0.5$ as well as $Sr_3Ru_2O_7$ exhibit FM or metamagnetic transitions with sizeable moments [44, 62]. In these truly FM compounds the magnetic fluctuations also differ from the FM paramagnon response and retain a small-q incommensurate AFM character [63–66], although the q width in these materials is much smaller than that of the qFM part in Sr_2RuO_4. The qFM signal in Sr_2RuO_4 exhibits a characteristic energy that is only a little larger than that of the IC signal, supporting the notion that Sr_2RuO_4 is also close to FM order [43, 44].

To access the role of the qFM fluctuations in the SC pairing we apply a simple weak-coupling approach relating the spin-mediated pairing interaction $V(\mathbf{k},\mathbf{k}')$ to the full $\chi(\mathbf{q},E)$, see, e.g. Ref. [67]: $\lambda\Delta(\mathbf{k}) = \sum_{\mathbf{k}'} V(\mathbf{k},\mathbf{k}')\cdot\Delta(\mathbf{k}')$, where $\Delta(\mathbf{k})$ characterizes the SC order parameter (SOP). $V(\mathbf{k},\mathbf{k}')$ is, for the singlet and triplet pairings [67]:

$$V_s(\mathbf{q}=\mathbf{k}-\mathbf{k}') = -3I^2(\mathbf{q})\chi'(\mathbf{q},0)\frac{1}{\sqrt{v_F(\mathbf{k})v_F(\mathbf{k}')}} \quad (3)$$

$$V_t(\mathbf{q}=\mathbf{k}-\mathbf{k}') = I^2(\mathbf{q})\chi'(\mathbf{q},0)\frac{|\hat{\mathbf{v}}_F(\mathbf{k})\cdot\hat{\mathbf{v}}_F(\mathbf{k}')|}{\sqrt{v_F(\mathbf{k})v_F(\mathbf{k}')}}$$

where $I(\mathbf{q})$ is defined as $I(q) = \chi_0(\mathbf{q})^{-1} - \chi(\mathbf{q})^{-1}$, and $\chi_0(\mathbf{q})$ is the noninteracting (Lindhardt) susceptibility. Note that only the amplitude of the single-relaxor spectra, $\chi'(\mathbf{q},0)$, enters the interaction matrices in this simple model. We use the tight binding Hamiltonian of Ref. [68] and parameterize the interaction as [10]: $I(\mathbf{q}) = I(0)/[1+b(\frac{a}{\pi})^2q^2]$, further details are given in [46]. The matrices $V_{s,t}(\mathbf{k},\mathbf{k}')$ are diagonalized by discretizing the Fermi surface into 1301 vectors $\mathbf{k}$. The largest eigenvalue of the interaction matrix defines the solution with the highest critical temperature, and the corresponding eigenvector defines the symmetry and the structure of the SOP. The interaction parameter $I(q)$ is crucial. Based on their calculations for $SrRuO_3$, Mazin and Singh [5, 10, 69] assigned the q dependence of I to the Hund's rule coupling on oxygen, and estimate $b = 0.08$. In the experiment, we find a much larger value $b = 0.44$, see Fig. 3(a), thus favoring more the triplet pairing.

We have diagonalized the matrices described by equation (3) using the two contributions separately, and using the total $\chi' = \chi'(\mathbf{q},0)$. The results are shown in Table I. As expected, for the IC fluctuations alone singlet solutions are most stable, and the qFM ones give triplets. With the total susceptibility, the IC fluctuations significantly contribute to the triplet solution as well, but the most stable state is still a singlet: the ratio of the largest singlet to the largest triplet eigenvalue is rather high, $R_{s/t}$ =4.8 [52]. Even a five times larger qFM part (clearly incompatible with the experiment) only reduces the ratio to $R_{s/t}$=1.4. Sharpening the parameter $I(q)$ significantly helps the triplet case, but not enough; tripling b to 1.32 only reduces $R_{s/t}$ to 2.2. Fig. 3 (c) and (d) present the SOPs for the most stable singlet and triplet solutions with the experimental set of parameters. The triplet solution is degenerate with the one rotated by 90°, so that a chiral state can be constructed. Note that both solutions have strong angular anisotropies (even vertical line nodes), not imposed by the p or d symmetries.

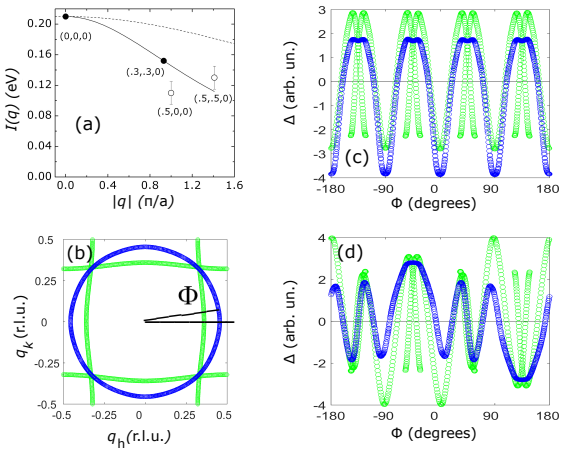

FIG. 3: (a) The interaction $I(\mathbf{q}) = I(0)/[1+b(\frac{a}{\pi})^2q^2]$ for b=0.08 (dashed line) and b=0.44 (solid line) compared with the experimental estimates; (b) 2D Fermi surface of Sr_2RuO_4 with the q1D (green) and q2D (blue) sheets; (c,d) SC order parameter on these sheets plotted against the angle with respect to the k_x-axis for the most stable singlet (c) and triplet (d) solutions.

In conclusion, we have identified the long-sought qFM fluctuations in Sr_2RuO_4, and, by comparing with the phonon scattering, quantitatively determined their amplitude. Combining this qFM signal and the nesting-driven IC response we have constructed the total magnetic susceptibility $\chi''(\mathbf{q},E)$ at all $\mathbf{q}$, which is consistent with the macroscopic susceptibility, with the specific heat coefficient in the normal state and with the $1/T_1T$ NMR results. Even though the experimentally determined qFM response is stronger and sharper than thought before, the IC component still dominates the spin-fluctuation spectrum in Sr_2RuO_4, so that the total susceptibility favors a singlet order parameter for simple spin-fluctuation mediated pairing. Thus, if the superconductivity in Sr_2RuO_4 is triplet, interactions beyond spin-fluctuation exchange would be required for the pairing mechanism.

This work was supported by the Deutsche Forschungs-

gemeinschaft through CRC 1238 Project No. B04 and by the JSPS KAKENHI No. 15H05852. I.I.M. was supported by ONR through the NRL basic research program.

* Electronic address: [e-mail:]braden@ph2.uni-koeln.de

[1] Y. Maeno, H. Hashimoto, K. Yoshida, S. Nishizaki, T. Fujita, J. G. Bednorz and F. Lichtenberg, Nature **372**, 532 (1994).

[2] A. P. Mackenzie and Y. Maeno, Rev. Mod. Phys. **75**, 657 (2003).

[3] Y. Maeno, S. Kittaka, T. Nomura, S. Yonezawa and K. Ishida, J. of Phys. Soc. Jpn. **81**, 011009 (2012).

[4] T. M. Rice and M. Sigrist, J. Phys. Condens. Matter **7**, L643 (1995).

[5] I. Mazin and D. Singh, Phys. Rev. Lett. **79**, 733 (1997).

[6] I. I. Mazin and D. J. Singh, Phys. Rev. **B56**, 2556 (1997).

[7] C. Kallin, Rep. Prog. Phys. 75, 042501 (2012).

[8] C. Kallin and A. Berlinsky, Rep. Prog. Phys. **79**, 054502 (2016).

[9] A. P. Mackenzie, T. Scaffidi, C. W. Hicks and Y. Maeno, npj Quantum Materials **2**, 40 (2017).

[10] I. Mazin and D. Singh, Phys. Rev. Lett. **82**, 4324 (1999).

[11] Y. Sidis, M. Braden, P. Bourges, B. Hennion, S. NishiZaki, Y. Maeno, and Y. Mori, Phys. Rev. Lett. **83**, 3320 (1999).

[12] T. Nomura and K. Yamada, J. Phys. Soc. Jpn. 69, 3678 (2000).

[13] T. Nomura and K. Yamada, J. Phys. Soc. Jpn. 71, 404 (2002).

[14] S. Raghu, A. Kapitulnik and S. A. Kivelson, Phys. Rev. Lett. **105**, 136401 (2010).

[15] T. Takimoto, Phys. Rev. B **62**, 14641(R) (2000).

[16] M. Tsuchiizu, Y. Yamakawa, S. Onari, Y. Ohno, and H. Kontani, Phys. Rev. B **91**, 155103 (2015).

[17] J.W. Huo, T.M. Rice and F.-C. Zhang, Phys. Rev. Lett. **110**, 167003 (2013).

[18] T. Scaffidi, and S. H. Simon, Phys. Rev. Lett. **115**, 087003 (2015).

[19] C. Bergemann, A. Mackenzie, S. Julian, D. Forsythe, and E. Ohmichi, Adv. in Phys. **52**, 639 (2003).

[20] C. N. Veenstra, Z.-H. Zhu, M. Raichle, B. M. Ludbrook, A. Nicolaou, B. Slomski, G. Landolt, S. Kittaka, Y. Maeno, J. H. Dil, I. S. Elfimov, M. W. Haverkort and A. Damascelli, Phys. Rev. Lett. **112**, 127002 (2014).

[21] M. Kim, J. Mravlje, M. Ferrero, O. Parcollet, and A. Georges, Phys. Rev. Lett. **120**, 126401 (2018).

[22] Y. Maeno, K. Yoshida, H. Hashimoto, S. Nishizaki, S-I. Ikeda, M. Nohara, T. Fujita, A. P. Mackenzie, N. E. Hussey, J. G. Bednorz, et al., J. Phys. Soc. Japan **66**, 1405 (1997).

[23] T. Oguchi, Phys. Rev. B **51**, 1385 (1995).

[24] D. Singh, Phys. Rev. B **52**, 1358 (1995).

[25] I. Hase and Y. Nishihara, J. Phys. Soc. Japan **65**, 3957 (1996).

[26] M. Braden, Y. Sidis, P. Bourges, P. Pfeuty, J. Kulda, Z. Mao,and Y. Maeno, Phys. Rev. B **66**, 064522 (2002).

[27] F. Servant, B. Fak, S. Raymond, J. P. Brison, P. Lejay, and J. Flouquet, Phys. Rev. B **65** , 184511 (2002).

[28] A. Liebsch, A.I. Lichtenstein, Phys Rev Lett. **84**, 1591 (2000).

[29] J. Mravlje, M. Aichhorn, T. Miyake, K. Haule, G. Kotliar, and A. Georges, Phys. Rev. Lett. **106**, 096401 (2011).

[30] M. Braden, P. Steffens, Y. Sidis, J. Kulda, P. Bourges, S. Hayden, N. Kikugawa, and Y. Maeno, Phys. Rev. Lett. **92**, 097402 (2004).

[31] K. Iida, M. Kofu, N. Katayama, J. Lee, R. Kajimoto, Y. Inamura, M. Nakamura, M. Arai, Y. Yoshida, M. Fujita, K. Yamada, and S.-H. Lee Phys. Rev. B **84**, 060402(R) (2011).

[32] K. Iida, J. Lee, M. B. Stone, M. Kofu, Y. Yoshida, and S.-H. Lee, J. of Phys. Soc. Jpn. **81**, 124710 (2012).

[33] S. Kunkemöller, P. Steffens, P. Link, Y. Sidis, Z. Mao, Y. Maeno, and M. Braden, Phys. Rev. Lett. **118**, 147002 (2017).

[34] M. Minakata and Y. Maeno, Phys. Rev. B **63**, 180504(R) (2001).

[35] M. Braden, O. Friedt, Y. Sidis, P. Bourges, M. Minakata and Y. Maeno, Phys. Rev. Lett. **88**, 197002 (2002).

[36] J.P. Carlo, T. Goko, I. M. Gat-Malureanu, P. L. Russo, A. T. Savici, A. A. Aczel, G. J. MacDougall, J. A. Rodriguez, T. J. Williams, G. M. Luke, C. R. Wiebe, Y. Yoshida, S. Nakatsuji, Y. Maeno, T. Taniguchi and Y. J. Uemura, Nature Materials **11**, 323 (2012).

[37] S. Kunkemöller, A. A. Nugroho, Y. Sidis and M. Braden, Phys. Rev. B **89**, 045119 (2014).

[38] M. Sato and M. Kohmoto, J. of Phys. Soc. Jpn. **69**, 3505 (2000).

[39] T. Kuwabara and M. Ogata, Phys. Rev. Lett. **85**, 4586 (2000).

[40] K. Kuroki, M. Ogata, R. Arita, and H. Aoki, Phys. Rev. B **63**, 060506(R) (2001).

[41] K. Ishida, H. Mukuda, Y. Kitaoka, Z. Q. Mao, H. Fukazawa, and Y. Maeno, Phys. Rev. B **63**, 060507 (2001).

[42] K. Ishida, H. Mukuda, Y. Minami, Y. Kitaoka, Z. Q. Mao, H. Fukazawa, and Y. Maeno, Phys. Rev. B **64**, 100501 (2001).

[43] J. E. Ortmann, J. Y. Liu, J. Hu, M. Zhu, J. Peng, M. Matsuda, X. Ke, and Z. Q. Mao, Scientific Reports **3**, 2950 (2013).

[44] S. Nakatsuji, D. Hall, L. Balicas, Z. Fisk, K. Sugahara, M. Yoshioka, and Y. Maeno, Phys. Rev. Lett. **90**, 137202 (2003).

[45] Z.Q. Mao, Y. Maeno, H. Fukazawa, Materials research bulletin **35**, 1813 (2000).

[46] In the supplemental material **** further information about the polarized INS experiments and about the calculations is given. In addition unpolarized INS data and polarized data at 150 K is presented as well as a quantitative comparision with NMR and specific heat experiments.

[47] M. Braden, W. Reichardt, S. Nishizaki, Y. Mori, and Y. Maeno, Phys. Rev. B **57**, 1236 (1998).

[48] M. Braden, W. Reichardt, Y. Sidis, Z. Mao, and Y. Maeno, Phys. Rev. B **76**, 014505 (2007).

[49] As a result of subtracting similar count rates, the resulting error bars are relatively large (see Fig. 1). The BG contains an essential part that depends only on the scattering angle. By analyzing many **Q** scans, a BG function depending on the scattering angle could be fitted. The variation of the BG also reflects the variation of the nSF count rates indicating that this part of the BG arises from

the finite flipping efficiency. Although in the analysis of the magnetic signals, the size of the magnetic scattering has almost exclusively been obtained from the PA, these considerations show that the BG is well understood and properly mastered.

[50] N. Qureshi, P. Steffens, D. Lamago, Y. Sidis, O. Sobolev, R. A. Ewings, L. Harnagea, S. Wurmehl, B. Büchner, and M. Braden, Phys. Rev. B **90**, 144503 (2014).

[51] T. Moriya, *Spin Fluctuations in Itinerant Electron Magnetism* (Springer-Verlag Berlin Heidelberg, 1985).

[52] The overestimation of $\chi'(0,0)$ seems to arise from the IC Lorentzian tails. The data can be equally well described assuming a Gaussian decay also for the IC amplitude, with the parameters $\chi'_{\rm IC}$ = 214 μ_B/eV^2, W=0.12 *r.l.u.* and a constant $\Gamma_{\rm IC}$=11 meV. With this description there is no contribution of IC parts to **q**=0, but the results for the BCS eigenvalue calculation are nearly unchanged. In particular the singlet is still favoured with an eigenvalue (in units of Table I) of 78 compared to 20 for the triplet solution; $R_{s/t}$=3.9. Note that our analysis together with the macroscopic $\chi'(0,0)$ values excludes an essential high-energy qFM contribution beyond the range of our INS experiments.

[53] A. Zheludev, reslib 3.4c, Oak Ridge National Laboratory, Oak Ridge, TN, 2006.

[54] T. Imai, A. Hunt, K. Thurber, and F. Chou, Phys. Rev. Lett. **81**, 3006 (1998).

[55] C. Berthier, M. Julien, M. Horvati, and Y. Berthier, J. Phys. I France **6**, 2205 (1996).

[56] H. Mukuda, K. Ishida, Y. Kitaoka, K. Asayama, Z. Mao, Y. Mori, and Y. Maeno, J. Phys. Soc. Japan **67**, 3945 (1998).

[57] K. Ishida, Y. Kitaoka, K. Asayama, S. Ikeda, S. Nishizaki, Y. Maeno, K. Yoshida, and T. Fujita, Phys. Rev. B **56**, R505 (1997).

[58] D. M. Edwards and G. G. Lonzarich, Philosophical Magazine **65**, 1185 (1992).

[59] M. Hatatani and T. Moriya, J. Phys. Soc. Japan **64**, 3434 (1995).

[60] Q. H. Wang, C. Platt, Y. Yang, C. Honerkamp, F. C. Zhang, W. Hanke, T. M. Rice, and R. Thomale, EPL **104**, 17013 (2013).

[61] L. Boehnke, P. Werner, and F. Lechermann, EPL **122**, 57001 (2018).

[62] R. S. Perry, L. M. Galvin, S. A. Grigera, L. Capogna, A. J. Schofield, A. P. Mackenzie, M. Chiao, S. R. Julian, S. I. Ikeda, S. Nakatsuji, Y. Maeno, and C. Pfleiderer, Phys. Rev. Lett. **86**, 2661 (2001).

[63] O. Friedt, P. Steffens, M. Braden, Y. Sidis, S. Nakatsuji, and Y. Maeno, Phys. Rev. Lett. **93**, 147404 (2004).

[64] P. Steffens, Y. Sidis, P. Link, K. Schmalzl, S. Nakatsuji, Y. Maeno, and M. Braden, Phys. Rev. Lett. **99**, 217402 (2007).

[65] P. Steffens, O. Friedt, Y. Sidis, P. Link, J. Kulda, K. Schmalzl, S. Nakatsuji, and M. Braden, Phys. Rev. B **83**, 054429 (2011).

[66] L. Capogna, E. M. Forgan, S. M. Hayden, A. Wildes, J. A. Duffy, A. P. Mackenzie, R. S. Perry, S. Ikeda, Y. Maeno, and S. P. Brown Phys. Rev. B **67**, 012504 (2003).

[67] I. Eremin, D. Manske, S. G. Ovchinnikov, and J. F. Annett, Ann. Phys. **13**, 149 (2004).

[68] S. Okamoto and A. J. Millis, Phys. Rev. B **70**, 195120 (2004).

[69] I. Mazin and D. Singh, J. Phys. Chem. Solids **59**, 2185 (1998).